Effect of the functionalisation agent on the surface-enhanced Raman scattering (SERS) spectrum: Case study of pyridine derivatives

Elodie Dumont[a]*, Charlotte De Bleye[a], Merzouk Haouchine[a], Laureen Coïc[a], Pierre-Yves Sacré[a], Philippe Hubert[a], Eric Ziemons[a]

[a] University of Liege (ULiege), CIRM, VibraSanté Hub, Department of Pharmacy, Laboratory of Pharmaceutical Analytical Chemistry, CHU, B36, B-4000 Liege, Belgium.

[*] **Corresponding author**: E. Dumont, University of Liege (ULiege), CIRM, Vibra-Santé Hub, Department of Pharmacy, Laboratory of Pharmaceutical Analytical Chemistry, CHU, B36, B-4000 Liege, Belgium

Fax: +32-43.66.43.17 Phone: +32-43.66.43.24 E-mail address: elodie.dumont@uliege.be

Abstract

Nowadays, the use of functionalised surface-enhanced Raman scattering (SERS) substrates has become very common. These surface modifying agents notably act as Raman reporters, as sensors of biological processes (pH, redox probes) or to increase the sensitivity and/or the specificity of SERS detections.

However, the effects of the functionalisation agents are deeply examined in very few studies, even though they can affect the aggregation behaviour of the SERS substrate. Moreover, depending on their concentration and on the pH, their spectral signature can be modified and they can even degrade if stored inappropriately.

In this context, this paper aims at emphasising the importance of the different aspects previously listed in the selection of a functionalisation agent. Pyridine derivatives were picked out to highlight these parameters, as some of these compounds are commonly used to be grafted onto SERS substrates. Two widespread syntheses of nanoparticles were selected as SERS substrates: citrate-reduced gold and silver nanoparticles. The surface of the nanoparticles was functionalised with several pyridine derivatives at different concentrations and in several solvents. It was observed that the molecules under study had a concentration-dependent effect on nanoparticle aggregation. A stability study was furthermore conducted in order to determine the best preservation conditions of the grafting solutions.

In conclusion, this paper shines a light on the relevance of the investigation of the too-often neglected behaviour of the surface modifying agents. Before their application in SERS analyses, parameters such as the label concentration should therefore be included in an experimental design to optimise the sample preparation.

Keywords: Surface-enhanced Raman scattering (SERS); Functionalization agents; Pyridine derivatives; Aggregation; Stability.

1. Introduction

Surface-enhanced Raman scattering (SERS) is currently booming in various research areas, such as the pharmaceutical and biomedical fields [1,2]. This can be explained by the numerous advantages of this vibrational technique: fast data acquisition, non-destructive measurements, qualitative, quantitative, multiplex and imaging capabilities and the compatibility with aqueous samples, among others. The use of label-free SERS substrates is being gradually shifted towards surface-modified SERS substrates. These allow to increase the complexity of the SERS detection, in compliance with intricate matrices that are nowadays analysed. Indeed, surface modifications improve the SERS substrates in different aspects [3-8]. They can increase nanoparticle biocompatibility and stability by conferring anti-fouling or anti-aggregation properties. They can also be used to tune the surface plasmon absorbance peak of the substrate in order to match it with the laser wavelength. Moreover, they can improve the specificity and sensitivity of the SERS detection, since specific recognition elements (aptamers, antibodies, molecularly imprinted polymer) can be grafted on the substrate surface. Additionally, when they are used as internal standards or to control the formation of hot-spots, the repeatability of SERS analyses is enhanced. Imaging and multiplex detections are also enabled by the use of Raman reporters. Finally, functionalisation of the substrate surfaces can be used in theoretical SERS studies, e.g. in order to improve the comprehension of SERS enhancement mechanisms. The reader interested in applications of functionalised SERS substrates, in environment science, food-processing or in the biomedical field, can find more information in reviews [3-8]. Some concrete examples of biomedical applications include the functionalisation of silver nanoparticles with pyridine in order to increase the sensitivity of detection of bisphenols, which are well-known endocrine disruptors found in tap water and in cash receipts [9]. Functionalised SERS substrates have been used to monitor the localisation of nanoparticles into cells by SERS imaging [10,11], and SERS-based immunoassays exploit the use of functionalised substrates as target molecule binding readout [12]. A last example is the use of grafted molecules as probes to monitor biological processes, such as the intracellular pH [13], the intracellular redox state [14] or the tissue production of NO [15].

It is a common practice to graft small aromatic molecules having a thiol or an amine in their structure onto SERS substrates, since these chemical functions present the advantage of covalently binding to metallic surfaces. This leads to stable chemical bonds and to high SERS signals. In contrast, physisorbed Raman labels tend to detach from the SERS surface over time

when placed in complex media [11]. The selection of a particular label depends on its purpose, but general structure rules involve a small size, symmetry in the structure and a high cross-section in order to keep the SERS signal of the label molecule as simple and intense as possible, with few characteristic bands [2]. These bands must be located at spectral positions generating no or the least interference with the sample analysed. As such, SERS substrates functionalised with alkyne or nitrile molecules have for example been used because the alkyne and nitrile bonds are situated in the biological silent region of the SERS spectrum [16,17].

Notwithstanding that surface functionalisation agents are widely applied in SERS, a recurrent shortage has been noticed about the preliminary study of the SERS label properties such as their stability or the impact of their concentration on the SERS signal intensity obtained as well as on the position of their characteristic bands. More generally, this observation takes place in the context of a lack of rational and reproducible optimisation of SERS experimental conditions. Little literature can indeed be found on experimental designs applied to SERS even though the design of experiments (DoE) approach is time-saving and allows to fully exploit the interdependence between the numerous parameters that can influence the SERS response [18-26]. Among these parameters, careful consideration must be given to the substrate, the type and concentration of the aggregation and surface modification agents, as well as to the pH and incubation time of the sample, since they are critical to the magnitude of the SERS response. The absence of rational optimisation often results in sub-optimal and seldom repeatable sample preparations.

Accordingly, in order to start remedying this shortage problem, we focussed on some pyridine derivatives, namely 2- and 4-mercaptopyridine (2-MP, 4-MP) and 2- and 4-pyridylethylmercaptan (2-PEM, 4-PEM), and analysed the effect of the concentration of these SERS labels on the SERS spectra and on the aggregation behaviour of the SERS substrates. These substrates consisted of suspensions of citrate-reduced gold and silver nanoparticles synthesised according to the Lee and Meisel protocol [27] since they are commonplace. The functionalisation agents were chosen because 2-MP and 4-MP have frequently been grafted onto SERS substrates to perform SERS analyses and to value the SERS enhancement factors of new substrates [11,13,28-30]. 2-PEM and 4-PEM were added to scrutinize the effect of small structural changes on the SERS response. To have an overview of thiolated pyridine labels, the SERS response and the aggregation behaviour of pyridine- and thiophenol-functionalised nanoparticles was also examined. For 2-MP and 4-MP, the effect of the solvent was moreover

looked at, since solvent-analyte and solvent-substrate interactions can impact the SERS response, in terms of intensity and band position, due to different surface adsorption geometries [31]. Finally, the selected labels being unstable, a UV-Visible stability study was carried out in order to underline the importance of the right preservation conditions of the SERS label solutions.

The results obtained in this study brought to light that the label concentration was critical regarding the aggregation state of the SERS substrates and for the SERS spectra obtained. The metal nature of the SERS substrate, as well as the solvent used to prepare the label solutions had also a great importance, especially on the sensitivity of the detection. Besides, the structure of the label was crucial since small structural variations could lead to a drop in sensitivity.

Consequently, it should be recommended to include parameters related to the surface modification agent in an experimental design during the development of any SERS experimental protocol, in order to optimise it. The SERS label properties are indeed critical to the SERS response and are interdependent with other parameters such as the aggregation agent. Without aiming at answering all the observation made during our study, we hope that this paper will raise awareness of the insufficient SERS label investigation problem among the SERS scientific community.

2. Materials and methods

2.1 *Chemicals and reagents*

Gold(III) chloride hydrate (99.995% trace metals basis), 2-mercaptopyridine (99%, ReagentPlus, 2-MP), 4-mercaptopyridine (95%, 4-MP), 2-pyridylethylmercaptan (2-PEM), 4-pyridylethylmercaptan (4-PEM), benzenethiol (99+%, TPh), pyridine (anhydrous, 99.8%, Pyr) were obtained from Sigma-Aldrich (St. Louis, MO, USA). Absolute ethanol (for analysis) and hydrochloric acid (37%, for analysis) were acquired from VWR Chemicals (Leuven, Belgium). Trisodium citrate (anhydrous, 98%) was purchased from Acros Organics (Geel, Belgium). Merck (Darmstadt, Germany) was the supplier of nitric acid (65%, for analysis) and silver nitrate (crystals, extra pure). Methanol (Ultra, HPLC-UHPLC grade) was acquired from J.T. Baker (Sowinskiego, Poland). All chemicals were used as received. Ultrapure water with a resistivity of 18.2 MΩcm was generated from a Milli-Q device (Millipore, Bellirica, MA, USA).

2.2 *Nanoparticle synthesis*

Citrate-coated gold and silver nanoparticles (AuNPs and AgNPs) were synthesized according to the method described by Lee and Meisel [27]. Each batch was characterised in terms of size, size dispersion and surface charge. The detailed synthesis and characterisation protocols can be found in references [18,19]. NPs were kept in the fridge and sheltered from light in order to guarantee their long-term stability. To ensure results were not caused by variations in NPs properties, the same batch of AuNPs and AgNPs was used to conduct all experiments. Moreover, all SERS experiments were done over 2 days whereas all DLS measurements were conducted over a week. In total, the entire NPs study lasted less than 3 weeks.

2.3 *Solution preparation*

Stock solutions of 2-MP, 4-MP and Pyr were prepared at a concentration of 10 mM in ultrapure water and were subsequently diluted with the same solvent. 10 mM 2-MP, 4-MP, 2-PEM and 4-PEM stock solutions were prepared and further diluted with methanol. A 10 mM stock solution of TPh was prepared and diluted in ethanol.

For UV-Visible spectroscopy, aliquots of 0.1 mM solutions of 2-MP and 4-MP in water and in methanol and of 0.2 mM solutions of 2-PEM and 4-PEM in methanol were stored both at room temperature with sunlight exposure and in the fridge sheltered from light.

2.4 *Equipment*

The SERS spectra were acquired on a LabRAM HR Evolution Raman microscope (Horiba Jobin-Yvon, Lyon, France) equipped with a 785 nm laser (50 mW on the sample), a two-dimensional EMCCD detector (1600 x 200 pixels sensor), a 300 gr/mm grating and a 50x LWD objective (NA = 0.55). The data were collected from 350 to 1750 cm^{-1} with a confocal slit-hole of 200 µm. Three acquisitions of 3 s were realised on the samples, which were prepared by vortexing 400 µL of NPs with 50 µL of functionalisation agent during 3 s.

The hydrodynamic diameter and the Zeta potential of functionalised NPs were measured with a Zetasizer Nano ZS (Malvern Instruments, Malvern, UK) operating at 25°C and equipped with a 633 nm He-Ne laser. The signal was collected at a 173° angle (non-invasive back-scatter system). The suspensions of NPs were diluted 10 times with ultrapure water before analysis.

For the stability study conducted in UV-Visible spectroscopy, a Lambda 40 UV-Visible spectrophotometer (Perkin Elmer, Waltham, MA, USA) was used. The samples were put in a 10 mm quartz cuvette and the UV-Visible spectra were acquired from 190 to 450 nm with a spectral resolution of 1 nm. Depending on the solvent used to prepare the sample, ultrapure water or methanol was used as blank sample in order to subtract the solvent background.

2.5 *Data analysis*

The SERS data were analysed with Matlab R2018a (The Mathworks, Natick, MA, USA) and the PLS_Toolbox 8.6.2 (Eigenvector Research, Inc., Wenatchee, WA, USA). An automatic Whittaker filter ($\lambda = 100000$, $p = 0.001$) was applied to correct the baseline of the SERS spectra.

3. Results and discussion

3.1 *SERS spectra and effect on the aggregation*

The first step when studying a new SERS functionalisation agent is the determination of the characteristic bands of the latter, and therefore the exploitable bands in the spectrum of this agent. Then, the optimal concentration of the label must be determined simultaneously with the nature and the concentration of the aggregation agent and the pH, as these parameters often experience interdependency [20].

This study focused on 2-MP, 4-MP, 2-PEM and 4-PEM, which can all covalently bind to metallic surfaces through their sulphur and/or nitrogen atom(s) [32-36]. Consequently, this theoretically results in a native affinity towards the SERS substrates and in high SERS signals. Since the structure of these molecules include a pyridine ring and a thiol, Pyr and TPh were also analysed in order to examine the relative contributions of these structure elements to the behaviour of the pyridine derivatives. Additionally, 2-MP and 4-MP were prepared in two different solvents, water and methanol, in order to investigate any possible solvent impact on the SERS response. Fig. S1 (Supporting Information) illustrates the structure of the different molecules studied.

The SERS spectra of these surface modifying agents were obtained by simply mixing them with the NPs, since it was observed that the functionalisation agents aggregated the colloids. The SERS spectra of the different grafting agents, at several concentrations, are displayed in the Supporting Information (Figs. S2-S17 (Supporting Information)). This aggregation effect was concentration dependent, with lower concentrations generating less aggregation. Table 1 summarises the influence of the functionalisation agent concentration on the SERS intensities. Colloid aggregation triggered by the functionalisation agent is a fact of which one must be well aware before starting the fulfilment of the SERS analyses. Indeed, in some cases, it may be interesting to use pre-aggregated nanoparticles [18] while in other applications the functionalised suspensions are required to remain stable over time [11,13-15]. The concentration of the grafting agent must therefore be adapted in accordance with the requirement of the experimental design.

These observations emphasise the fact that it is crucial to add the functionalisation agent component in the SERS method optimisation design in addition to that of the aggregation agent,

since both affect the aggregation state of the colloid. The difference in behaviour of 4-MP and 4-PEM related to 2-MP and 2-PEM (Table 1) also illustrates how importantly small structural changes can have repercussions on the SERS response.

In contrast to the aggregation obtained with AuNPs, the addition of 4-MP (both in water and in methanol), of 4-PEM and of Pyr to AgNPs failed to aggregate AgNPs (Table 1, Table S1), demonstrating the influence of the SERS substrate nature. However, despite the lack of AgNPs aggregation, weak SERS signals could be collected for AgNPs functionalised with 4-MP, even at quite low concentrations (µM range, Table 1). On the opposite, AgNPs functionalised with 4-PEM or Pyr failed to produce a SERS response at low (µM) concentrations (Table 1). Further investigations, such as molecular modelling, would be required to explain these phenomena.

The influence of the metallic nature of the NPs (gold or silver) on the SERS signal intensity could further be highlighted. AuNPs led to more sensitive results than AgNPs in terms of SERS visualisation of the functionalisation agent bands. This could be explained by the relative strength of metal-S and metal-N bonds, being stronger for gold than for silver [37,38]. The lower affinity of pyridine for AuNPs in comparison to 2-MP, 4-MP, 2-PEM and 4-PEM could also be interpreted according to the Au-N bond strength, which is weaker than the Au-S one [37]. Nonetheless, a difference in SERS efficacy resulting from discrepancies in NPs properties (size and concentration for instance) can not totally be ruled out, as these properties greatly influence susceptibility to aggregation. It is plausible though that the stronger the metal-bond is the easier aggregation will occur due to change in NPs surface environment.

A difference in the aggregation pattern of TPh compared to the other pyridine derivatives studied was observed (Fig. 1). While aggregation occurred instantly or did not occur at all for 2-MP, 4-MP, 2-PEM, 4-PEM and Pyr, aggregation took place more slowly at lower concentrations of TPh (lower than 0.1 mM). No SERS spectrum was observed for 1 and 0.5 µM TPh adsorbed onto AuNPs when AuNPs were directly analysed. However, after 45 min incubation, nanoparticle aggregation occurred and intense SERS spectra were thus obtained (Fig. 1a). This effect was less pronounced for AgNPs, where larger concentrations of TPh had to be used in order to obtain a SERS response. No SERS signal was observed for 100 and 50 µM TPh concentrations when analysed instantaneously, but after 5 min incubation time, the aggregation started occurring, with a TPh SERS signal increasing with time (Fig. 1b). However, even after 90 min incubation time, no SERS spectrum was obtained for 10 µM TPh. On one hand, once again, this lower sensitivity for AgNPs can be explained by the lower Ag-S bond

strength in comparison to the Au-S bond strength [38]. On the other hand, as studied by Tripathi *et al.* [39], the difference in the kinetics of appearance and of increase of the SERS spectra of TPh can also be explained by the pH of the NPs. AuNPs are acidic (pH 5.5) whereas AgNPs are basic (pH 8). At acidic pH, the thiol of TPh is mainly in the SH form, since its pKa is close to 7 [39], while at basic pH, it is mainly in the S^- form. Therefore, at basic pH, the sulphur is already deprotonated and the covalent binding of sulphur to the metal surface can occur faster than at acidic pH where deprotonation needs to occur first [39]. Since the pKa values of the thiol functions of 2-MP and 4-MP are lower than that of TPh [34,40], these functions are mainly in the S^- form. This could possibly explain the different behaviour observed with TPh and AuNPs. No effect of the incubation time was observed for all the other pyridine derivatives studied. This example of time-dependent aggregation behaviour highlights that the incubation time has to be taken into account during the development of the SERS method, especially when quantitative or semi-quantitative measurements are foreseen. Indeed, the signal intensity can depend both on time and on analyte concentration.

Additionally, the solvent effect on the SERS spectrum has to be born in mind. The small proportion of functionalisation agent used in this study (50 µL of pyridine derivatives mixed with 400 µL NPs) avoided any spectral interference originating from the solvent. Yet, if using larger amounts of SERS labels, some solvent bands could start appearing in the spectra. It was nevertheless noticed that the use of methanol instead of water slightly decreased the sensitivity of 2-MP and 4-MP detection, regardless of the NPs metal nature, because methanol stabilised slightly more the NPs suspensions. The influence of the solvent on the SERS substrate aggregation behaviour was thus shown to be significant. This additional parameter should consequently be taken into consideration during preliminary optimisation studies.

Minor differences were noticed in the SERS spectra of the same functionalisation agent analysed with the same kind of NPs, depending on the concentration of the surface modifying agent (spectra displayed in the Supporting Information). These differences mainly consisted in small band shifts and in inversion of band intensity ratios. This is not surprising, knowing that SERS is a surface sensitive technique. The orientation of the molecules adsorbed onto the surface of NPs will indeed be different whether they are densely or sparsely packed, consequently leading to modifications in the SERS spectra.

The AuNPs and AgNPs that were employed in this study present opposite pH characteristics, i.e. acidic for AuNPs (pH 5.5) and slightly basic (pH 8) for AgNPs. By contrasting the spectral

patterns obtained with AuNPs and AgNPs, it was finally interesting to examine the pH effect on the spectra of the pyridine derivatives. Indeed, the nitrogen belonging to the pyridine ring can be protonated or unprotonated in these derivatives according to the pH. For aqueous 2-MP (Fig. 2), the intensity ratio 1232/1273 cm^{-1} for AuNPs was higher than the ratio 1227/1275 cm^{-1} for AgNPs, which could indicate the more protonated state of the nitrogen in AuNPs in comparison to AgNPs [33]. The bands taken into account for these ratios are assigned to the out-of-plane deformation of NH/in-plane deformation of NH and to the stretching of C=C/C=N (mode number 14b), respectively [33]. For aqueous 4-MP (Fig. 3), the intensity ratios 1091/1000 cm^{-1} (respectively assigned to the 18a mode with C-S stretching and to the ring breathing mode 1 [34,41]) and 1570/1610 cm^{-1} (respectively assigned to the 8b2 ring stretching with deprotonated and protonated nitrogen [35,42]) were higher for AgNPs than for AuNPs. Furthermore, the band located around 1200 cm^{-1}, consisting of 2 overlapping bands for AuNPs, shifted towards higher wavenumbers while becoming a single well resolved band for AgNPs. The overlapping bands can be attributed to a combination of N-H deformation (at lower wavenumbers) and C-H in-plane bending (at higher wavenumbers) [41]. All these observations suggest a more protonated state of 4-MP adsorbed on AuNPs than on AgNPs [34,35,41,42]. Once again, this exemplifies the importance of including the sample pH parameter into the experimental design. Modifications of the pH can trigger band shifts or band ratio variations that could otherwise erroneously be attributed to an interaction of the grafting molecule with the analyte.

3.1.1 Dynamic and electrophoretic light scattering

Usually, dynamic and electrophoretic light scattering (DLS and ELS) are useful to assist in monitoring the efficiency of the SERS substrate coating process [43,44]. However, DLS and ELS can further be exploited in order to study the stability of the grafted SERS substrates. These analytical tools are consequently well suited to assist in SERS method development.

Therefore, the aggregation effect of the different pyridine derivatives on AuNPs and AgNPs was objectified by means of DLS and ELS measurements. The results of these measurements are summarised in Table 2 and in Table S1 (Supporting Information) and are consistent with the visual observations made about the aggregation behaviour of the functionalised colloids.

The native AuNPs and AgNPs suspensions were negatively charged, with a zeta potential around -44 and -45 mV respectively, due to the citrate layer adsorbed onto the NPs surface. The

suspensions had a mean hydrodynamic size of 90 and 46 nm respectively. An increase in the mean size of the NPs suspensions suggested appearance of NPs aggregates. A drop in the zeta potential conveyed an instability of the suspension brought about by the decrease of repulsive interactions between NPs. A common value of ± 30 mV is generally accepted as threshold for colloidal stability [45], i.e. suspensions with a zeta potential included between -30 mV and + 30 mV are considered unstable.

Samples that were partly aggregated were characterised by a slightly larger size and/or by a slightly less negative zeta potential. Indeed, a 1 to 2-fold size increase was noticed for partly aggregated samples, whereas a 1.5 to 7-fold increase was observed for the highly aggregated ones (Table S1 (Supporting Information)).

Regarding SERS, the aggregation of the colloidal substrate is required in order to form hot-spots, which are areas of the sample where the SERS signal is the most enhanced. These hot-spots occur at the junction of two or more aggregated nanoparticles. However, the SERS signal is also a compromise, as aggregated NPs will flocculate with time, hence bringing about large signal drops. The repeatability of SERS analyses will therefore be affected if the state of aggregation of the colloids varies over the course of an experiment. Consequently, it should be recommended to study the effect of incubation time on signal intensity and repeatability. This phenomenon can clearly be observed in Table 2. The most aggregated experimental conditions, determined by DLS and ELS (and depicted in Table S1 (Supporting Information)), did not lead to the highest SERS response. On the contrary, the best SERS signals were obtained for samples that were partly aggregated, thus more stable over time.

3.2 *UV-Visible stability study*

It is a well-known fact that 2- or 4-thiol-substituted pyridines are prone to tautomerization. The thione tautomers form preferably in solution and assemble in H-bonded dimers [33,34,46]. Moreover, thiol molecules are susceptible to form disulphide bridges by oxidation [46]. These molecular changes could modify the SERS spectrum of the SERS labels and/or the aggregation state of the colloid, potentially leading to misinterpretation of the results of SERS experiments. Therefore, monitoring of the stability of 2-MP, 4-MP, 2-PEM and 4-PEM solutions was carried out by UV-Visible spectroscopy.

For aqueous 2-MP and 4-MP, the same trend was observed: solutions kept in the fridge and shielded from light did not show any spectral variation up to 3 months (further time not tested). Conversely, the solutions stored at room temperature (RT) and in the sunlight started to display spectral changes after one day (Fig. 4). These changes consisted in a decrease of the intensity of the 271 and 342 nm peaks with the appearance of a peak at 231 nm for 2-MP. For 4-MP, the intensity of the peaks at 230 and 324 nm dropped with time and a large peak arose around 253 nm. In order to find out if the spectral modifications triggered by RT storage could be reversible, aliquots of 2-MP and 4-MP samples stored for 9 days at RT were further refrigerated. The peak intensities stopped decreasing although they did not return to the level of the samples kept in the fridge from the beginning of the stability study. It was thus hypothesised that the degradation process was prevented when the samples are stored in the fridge, but that the structural changes that had occurred during storage at RT were not reversible.

Since 2-MP and 4-MP are also soluble in methanol, the effect of this solvent on the stability of 2-MP and 4-MP was studied. It can be observed in Fig. 4 that the samples prepared in methanol followed the same trend as that prepared in water. No spectral change was noticed for the samples stored in the fridge. Variations in spectral intensities of RT-stored samples were on the opposite already coming out after one day. However, these variations seemed to occur more rapidly in methanol than in water. This led to the assumption that the stability of 2-MP and 4-MP was slightly worse in methanol than in water. The peak positions of 2-MP and 4-MP were shifted in methanol, due to the solvent effect on the UV-Visible spectra. On one hand, the 282 and 360 nm peak intensities of 2-MP decreased with the RT storage time, while a new peak appeared at 235 nm. On the other hand, the 4-MP peaks at 227, 295 and 337 nm lowered whereas a large peak appeared at 245 nm.

2-PEM and 4-PEM being insoluble in water, their stability was only monitored in methanol. In contrast to 2-MP and 4-MP, the UV-Visible spectra of 2-PEM and 4-PEM did not display any significant difference as a function of time and of the storage conditions (Figs. S18 and S19 (Supporting Information)).

3.2.1 SERS on stability study samples

The samples used for the UV-Visible stability study were in addition analysed by SERS, in order to assess whether the UV-Visible spectral changes were relevant when conducting SERS analyses.

In spite of distinct UV-Visible spectra, the SERS spectra obtained for aqueous 2-MP and 4-MP stored one month at RT with AuNPs and AgNPs did not display any significant differences (Figs. S20-23 (Supporting Information)). This could be readily explained by the disulphide bond cleavage of disulphide dimers, that dissociatively chemisorb onto gold and silver surfaces, regenerating the starting label molecules [47]. Nonetheless, a reduction in the aggregation could be noted, leading to a drop in the SERS intensity of AgNPs functionalised with 2-MP stored at RT compared with 2-MP kept in the fridge (Fig. S22 (Supporting Information)). A possible explanation can be found in the weaker strength of Ag-S and Ag-N bonds in comparison to Au-S and Au-N bonds, as previously stated [37,38], probably bringing less dissociative chemisorption about.

For methanolic solutions of 2-MP and 4-MP, similar results were obtained, except for 4-MP-grafted AuNPs, where a difference in aggregation behaviour (less pronounced for the solution kept at RT) and spectral changes were noticed (Fig. 5).

As their UV-Visible spectra did not show any change with time, it was not a surprise that the SERS spectra of 2-PEM and 4-PEM remained the same after 1 month storage at RT and in the fridge (Fig. S24-27).

4. Conclusion

This paper presented an in-depth study of some SERS labels belonging to the structural family of pyridine, with AuNPs and AgNPs that are commonly used by the SERS scientific community.

This work underlined the importance of carrying out an exhaustive study of the SERS label before its use in SERS analyses, which is currently too often neglected. Indeed, numerous parameters can interdependently impact the SERS detection. Among these parameters, it was demonstrated that the label structure and concentration, the SERS substrate metal nature, the pH, the solvent and the storage conditions affected the aggregation state of NPs and their SERS response.

To conclude, simultaneous investigation and optimisation of all these parameters before further use of the grafted NPs should be standard practice. In our opinion, the best methodology to that purpose is the DoE strategy, that thus merits receiving more attention in the SERS community.

Acknowledgements

The National Fund for Scientific Research, FNRS-F.R.S. is gratefully acknowledged for the Aspirant funding granted to E. Dumont (1.A030.17 – FC6921). This work was also supported by the Faculty of Medicine of the University of Liège (Crédits facultaires). The European funds of regional development (FEDER) and the Walloon Region program "Walloon-2020.EU" are also thanked for the funding of L. Coïc.

Appendix A. Supplementary data

Additional Supporting Information may be found online.

References

[1] J. Cailletaud, C. De Bleye, E. Dumont, P.-Y. Sacré, L. Netchacovitch, Y. Gut, M. Boiret, Y.-M. Ginot, Ph. Hubert, E. Ziemons, Critical review of surface-enhanced Raman spectroscopy applications in the pharmaceutical field, J. Pharm. Biomed. Anal. 147 (2018) 458-472. https://doi.org/10.1016/j.jpba.2017.06.056.

[2] E. Dumont, C. De Bleye, P.-Y. Sacré, L. Netchacovitch, Ph. Hubert, E. Ziemons, From near-infrared and Raman to surface-enhanced Raman spectroscopy: progress, limitations and perspectives in bioanalysis, Bioanalysis 8(10) (2016) 1077-1103. https://doi.org/10.4155/bio-2015-0030.

[3] T. Yaseen, H. Pu, D.-W. Sun, Functionalization techniques for improving SERS substrates and their applications in food safety evaluation: A review of recent research trends, Trends Food Sci. Technol. 72 (2018) 162-174. https://doi.org/10.1016/j.tifs.2017.12.012.

[4] C.K. Klutse, A. Mayer, J. Wittkamper, B.M. Cullum, Applications of self-assembled monolayers in surface-enhanced Raman scattering, J. Nanotechnol. 2012, 319038. http://dx.doi.org/10.1155/2012/319038.

[5] B. Shan, Y. Pu, Y. Chen, M. Liao, M. Li, Novel SERS labels: Rational design, functional integration and biomedical applications, Coord. Chem. Rev. 371 (2018) 11-37. https://doi.org/10.1016/j.ccr.2018.05.007.

[6] L. Rodriguez-Lorenzo, L. Fabris, R.A. Alvarez-Puebla, Multiplex optical sensing with surface-enhanced Raman scattering: A critical review, Anal. Chim. Acta 745 (2012) 10-23. https://doi.org/10.1016/j.aca.2012.08.003.

[7] P.C. Pinheiro, A.L. Daniel-da-Silva, H.I.S. Nogueira, T. Trindade, Functionalized inorganic nanoparticles for magnetic separation and SERS detection of water pollutants, Eur. J. Inorg. Chem. 30 (2018) 3443-3461. https://doi.org/10.1002/ejic.201800132.

[8] L. Fabris, Gold-based SERS tags for biomedical imaging, J. Opt. 17 (2015) 114002. https://doi.org/10.1088/2040-8978/17/11/114002.

[9] C. De Bleye, E. Dumont, C. Hubert, P.-Y. Sacré, L. Netchacovitch, P.-F. Chavez, Ph. Hubert, E. Ziemons, A simple approach for ultrasensitive detection of bisphenols by

multiplexed surface-enhanced Raman scattering, Anal. Chim. Acta 888 (2015) 118-125. https://doi.org/10.1016/j.aca.2015.07.023.

[10] M.K. Gregas, J.P. Scaffidi, B. Lauly, T. Vo-Dinh, Surface-enhanced Raman scattering detection and tracking of nanoprobes: Enhanced uptake and nuclear targeting in single cells, Appl. Spectrosc. 64 (2010) 858-866. https://doi.org/10.1366/000370210792081037.

[11] N.M.S. Sirimuthu, C.D. Syme, J.M. Cooper, Investigation of the stability of labelled nanoparticles for SE(R)RS measurements in cells, Chem. Commun. 47 (2011) 4099-4101. https://doi.org/10.1039/c0cc05723a.

[12] J. Smolsky, S. Kaur, C. Hayashi, S.K. Batra, A.V. Krasnoslobodtsev, Surface-enhanced Raman scattering-based immunoassay technologies for detection of disease biomarkers, Biosensors 7(1) (2017) 7. https://doi.org/10.3390/bios7010007.

[13] Y. Shen, L. Liang, S. Zhang, D. Huang, J. Zhang, S. Xu, C. Liang, W. Xu, Organelle-targeting surface-enhanced Raman scattering (SERS) nanosensors for subcellular pH sensing, Nanoscale 10(4) (2018) 1622-1630. https://doi.org/10.1039/c7nr08636a.

[14] L.E. Jamieson, A. Jaworska, J. Jiang, M. Baranska, D.J. Harrison, C.J. Campbell, Simultaneous intracellular redox potential and pH measurements in live cells using SERS nanosensors, Analyst 140 (2015) 2330-2335. https://doi.org/10.1039/c4an02365j.

[15] S. Han, J. Sun, J. Wang, W. Qian, J. Dong, A built-in surface-enhanced Raman scattering-active microneedle for sampling in vivo and surface-enhanced Raman scattering detection ex vivo of NO, J. Raman Spectrosc. 49 (2018) 1747-1755. https://doi.org/10.1002/jrs.5469.

[16] X. Qin, M. Lyu, Y. Si, J. Yang, Z. Wu, J. Li, Alkyne-based surface-enhanced Raman scattering nanoprobe for ratiometric imaging analysis of caspase 3 in live cells and tissues, Anal. Chim. Acta 1043 (2018) 115-122. https://doi.org/10.1016/j.aca.2018.09.009.

[17] Y. Shen, L. Liang, J. Zhang, Z. Li, J. Yue, J. Wang, W. Xu, W. Shi, S. Xu, Interference-free surface-enhanced Raman scattering nanosensor for imaging and dynamic monitoring of reactive oxygen species in mitochondria during photothermal therapy, Sens. Actuators B Chem. 285 (2019) 84-91. https://doi.org/10.1016/j.snb.2019.01.036.

[18] E. Dumont, C. De Bleye, J. Cailletaud, P.-Y. Sacré, P.-B. Van Lerberghe, B. Rogister, G.A. Rance, J.W. Aylott, Ph. Hubert, E. Ziemons, Development of a SERS strategy to overcome the nanoparticle stabilisation effect in serum-containing samples: Application to the quantification of dopamine in the culture medium of PC-12 cells, Talanta 186 (2018) 8-16. https://doi.org/10.1016/j.talanta.2018.04.038.

[19] C. De Bleye, E. Dumont, E. Rozet, P.-Y. Sacré, P.-F. Chavez, L. Netchacovitch, G. Piel, Ph. Hubert, E. Ziemons, Determination of 4-aminophenol in a pharmaceutical formulation using surface enhanced Raman scattering: From development to method validation, Talanta 116 (2013) 899-905. https://doi.org/10.1016/j.talanta.2013.07.084.

[20] H. Fisk, C. Westley, N.J. Turner, R. Goodacre, Achieving optimal SERS through enhanced experimental design, J. Raman Spectrosc. 47(1) (2016) 59-66. https://doi.org/10.1002/jrs.4855.

[21] D. Gloria, J.J. Gooding, G. Moran, D.B. Hibbert, Electrochemically fabricated three dimensional nanoporous gold films optimized for surface enhanced Raman scattering, J. Electroanal. Chem. 656 (2011) 114-119. https://doi.org/10.1016/j.jelechem.2010.12.028.

[22] R.M. Jarvis, W. Rowe, N.R. Yaffe, R. O'Connor, J.D. Knowles, E.W. Blanch, R. Goodacre, Multiobjective evolutionary optimisation for surface-enhanced Raman scattering, Anal. Bioanal. Chem. 397 (2010) 1893-1901. https://doi.org/10.1007/s00216-010-3739-z.

[23] C. Levene, E. Correa, E.W. Blanch, R. Goodacre, Enhancing surface enhanced Raman scattering (SERS) detection of propranolol with multiobjective evolutionary optimization, Anal. Chem. 84 (2012) 7899-7905. https://doi.org/10.1021/ac301647a.

[24] L.F. Sallum, F.L.F. Soares, J.A. Ardila, R.L. Carneiro, Optimization of SERS scattering by Ag-NPs-coated filter paper for quantification of nicotinamide in a cosmetic formulation, Talanta 118 (2014) 353-358. https://doi.org/10.1016/j.talanta.2013.10.039.

[25] S. Mabbott, E. Correa, D.P. Cowcher, J.W. Allwood, R. Goodacre, Optimization of parameters for the quantitative surface-enhanced Raman scattering detection of mephedrone using a fractional factorial design and a portable Raman spectrometer, Anal. Chem. 85 (2013) 923-931. https://doi.org/10.1021/ac302542r.

[26] B.R. Alvarenga Jr, F.L.F. Soares, J.A. Ardila, L.G.C. Durango, M.R. Forim, R.L. Carneiro, Determination of B-complex vitamins in pharmaceutical formulations by surface-enhanced

Raman spectroscopy, Spectrochim. Acta A Mol. Biomol. Spectrosc. 188 (2018) 589-595. https://doi.org/10.1016/j.saa.2017.07.049.

[27] P.C. Lee, D. Meisel, Adsorption and surface-enhanced Raman of dyes on silver and gold sols, J. Phys. Chem. 86 (1982) 3391-3395. https://doi.org/10.1021/j100214a025.

[28] T. Lou, Y. Wang, J. Li, H. Peng, H. Xiong, L. Chen, Rapid detection of melamine with 4-mercaptopyridine-modified gold nanoparticles by surface-enhanced Raman scattering, Anal. Bioanal. Chem. 401 (2011) 333-338. https://doi.org/10.1007/s00216-011-5067-3.

[29] E. Nalbant Esenturk, A.R. Hight Walker, Surface-enhanced Raman scattering spectroscopy via gold nanostars, J. Raman Spectrosc. 40 (2009) 86-91. https://doi.org/10.1002/jrs.2084.

[30] X.-Y. Zhu, A.-J. Wang, S.-S. Chen, X. Luo, J.-J. Feng, Facile synthesis of AgPt@Ag core-shell nanoparticles as highly active surface-enhanced Raman scattering substrates, Sens. Actuators B Chem. 260 (2018) 945-952. https://doi.org/10.1016/j.snb.2017.12.185.

[31] A. Tripathi, E.D. Emmons, N.D. Kline, S.D. Christesen, A.W. Fountain III, J.A. Guicheteau, Molecular structure and solvent factors influencing SERS on planar gold substrates, J. Phys. Chem. C 122 (2018) 10205-10216. https://doi.org/10.1021/acs.jpcc.8b00353.

[32] W.H. Do, C.J. Lee, D.Y. Kim, M.J. Jung, Adsorption of 2-mercaptopyridine and 4-mercaptopyridine on a silver surfaces investigated by SERS spectroscopy, J. Ind. Eng. Chem. 18 (2012) 2141-2146. https://doi.org/10.1016/j.jiec.2012.06.009.

[33] N. Hassan, R. Holze, Surface enhanced Raman spectroscopy of self-assembled monolayers of 2-mercaptopyridine on a gold electrode, Russ. J. Electrochem. 48(4) (2012) 401-411. https://doi.org/10.1134/S1023193512030056.

[34] H.S. Jung, K. Kim, M.S. Kim, Raman spectroscopic investigation of the adsorption of 4-mercaptopyridine on a silver-sol surface, J. Mol. Struct. 407 (1997) 139-147. https://doi.org/10.1016/S0022-2860(97)00006-9.

[35] H. Guo, L. Ding, Y. Mo, Adsorption of 4-mercaptopyridine onto laser-ablated gold, silver and copper oxide films: A comparative surface-enhanced Raman scattering investigation, J. Mol. Struct. 991 (2011) 103-107. https://doi.org/10.1016/j.molstruc.2011.02.012.

[36] K. Nishiyama, M. Tsuchiyama, A. Kubo, H. Seriu, S. Miyazaki, S. Yoshimoto, I. Taniguchi, Conformational change in 4-pyridineethanethiolate self-assembled monolayers on Au(111) driven by protonation/deprotonation in electrolyte solutions, Phys. Chem. Chem. Phys. 10 (2008) 6935-3939. https://doi.org/0.1039/b810777g.

[37] A. Bilic, J.R. Reimers, Adsorption of pyridine on the gold(111) surface: Implications for "alligator clips" for molecular wires, J. Phys. Chem. B 106 (2002) 6740-6747. https://doi.org/10.1021/jp020590i.

[38] S. Nath, S.K. Ghosh, S. Kundu, S. Praharaj, S. Panigrahi, T. Pal, Is gold really softer than silver? HSAB principle revisited, J. Nanopart. Res. 8 (2006) 111-116. https://doi.org/10.1007/s11051-005-8025-1.

[39] A. Tripathi, E.D. Emmons, S.D. Christesen, A.W. Fountain, J.A. Guicheteau, Kinetics and reaction mechanisms of thiophenol adsorption on gold studied by surface-enhanced Raman spectroscopy, J. Phys. Chem. C 117 (2013) 22834-22842. https://doi.org/10.1021/jp407105v.

[40] R.A. Jones, A.R. Katritzky, 721. Tautomeric pyridines. Part I. Pyrid-2- and -4-thione, J. Chem. Soc. 1958, 3610-3613. https://doi.org/10.1039/jr9580003610.

[41] H.-Z. Yu, N. Xia, Z.-F. Liu, SERS Titration of 4-mercaptopyridine self-assembled monolayers at aqueous buffer/gold interfaces, Anal. Chem. 71 (1999) 1354-1358. https://doi.org/10.1021/ac981131+.

[42] X.-S. Zheng, P. Hu, J.-H. Zhong, C. Zong, X. Wang, B.-J. Liu, B. Ren, Laser power dependent surface-enhanced Raman spectroscopic study of 4-mercaptopyridine on uniform gold nanoparticle-assembled substrates, J. Phys. Chem. C 118 (2014) 3750-3757. https://doi.org/10.1021/jp409711r.

[43] A.P. Ramos, Dynamic light scattering applied to nanoparticle characterization, in Nanocharacterization Techniques, (Eds: A.L. Da Roz, M. Ferreira, F. de Lima Leite, O.N. Oliveira Jr), Elsevier, United Kingdom, 2017, pp. 99-110.

[44] S. Liu, M. Lämmerhofer, Functionalized gold nanoparticles for sample preparation: A review, Electrophoresis 40 (2019) 2438-2461. https://doi.org/10.1002/elps.201900111.

[45] S. Bhattacharjee, DLS and zeta potential - What they are and what they are not?, J. Controlled Release 235 (2016) 337-351. https://doi.org/10.1016/j.jconrel.2016.06.017.

[46] S. Stoyanov, I. Petkov, L. Antonov, T. Stoyanova, P. Karagiannidis, P. Aslanidis, Thione–thiol tautomerism and stability of 2- and 4-mercaptopyridines and 2-mercaptopyrimidines, Can. J. Chem. 68 (1990) 1482. https://doi.org/10.1139/v90-227.

[47] M. Takahashi, M. Fujita, M. Ito, SERS application to some electroorganic reactions, Surf. Sci. 158 (1985) 307-313. https://doi.org/10.1016/0039-6028(85)90305-X.

Table 1: *Effect of the functionalisation agent concentration on the SERS intensity. The dark, medium and light grey boxes represent high, low and no SERS signal, respectively. Experimental conditions that were not tested are depicted by white boxes.*

Concentration	2-MP (water)		2-MP (MeOH)		4-MP (water)		4-MP (MeOH)		Pyr		2-PEM		4-PEM		TPh	
	AuNPs	AgNPs	AuNPs	AgNPs	AuNPs	AgNPs	AuNPs	AgNPs	AuNPs	AgNPs	AuNPs	AgNPs	AuNPs	AgNPs	AuNPs	AgNPs
0.1 µM																
0.5 µM																
1 µM																
2.5 µM																
5 µM																
10 µM																
25 µM																
50 µM																
0.1 mM																
1 mM																
5 mM																
10 mM																

Table 2: *Comparison of the SERS signal intensity in function of the aggregation state of NPs. The darker the boxes are, the more intense the SERS signal is. White boxes represent samples for which no SERS signal was obtained, whereas experimental conditions that were not tested are depicted by boxes containing a dash.*

Concentration		No functionalisation		2-MP (water)		2-MP (MeOH)		4-MP (water)		4-MP (MeOH)		Pyr		2-PEM		4-PEM		TPh	
		AuNPs	AgNPs	AuNPs	AgNPs	AuNPs	AgNPs	AuNPs	AgNPs	AuNPs	AgNPs	AuNPs	AgNPs	AuNPs	AgNPs	AuNPs	AgNPs	AuNPs	AgNPs
0 mM	Size (nm)	89.52	46.47	-	-	-	-	-	-	-	-	-	-	-	-	-	-	-	-
	Zeta (mV)	-44.00	-45.10																
1 µM	Size (nm)	-	-	93.20	47.15	93.16	-	90.71	46.82	93.07	47.12	-	-	92.43	46.91	93.36	48.08	95.23	47.71
	Zeta (mV)			-44.47	-44.50	-43.47		-46.40	-43.17	-43.47	-42.40			-41.63	-40.97	-41.63	-41.23	-41.30	-38.93
2.5 µM	Size (nm)	-	-	-	-	-	-	-	-	-	-	-	-	98.09	-	94.22	-	-	-
	Zeta (mV)													-40.17		-41.47			
10 µM	Size (nm)	-	-	134.73	46.79	150.70	48.48	113.93	48.05	116.87	47.50	-	-	147.97	48.47	137.10	47.14	93.10	48.29
	Zeta (mV)			-38.27	-45.27	-34.50	-42.03	-43.50	-45.07	-43.60	-42.93			-30.63	-36.60	-33.17	-40.73	-38.40	-40.17
50 µM	Size (nm)	-	-	-	-	-	80.42	-	-	-	-	-	-	-	47.25	-	-	-	47.79
	Zeta (mV)						-17.87								-27.50				-35.10
0.1 mM	Size (nm)	-	-	251.80	267.20	248.53	325.10	190.47	47.22	169.70	47.67	90.47	-	200.33	292.87	129.37	47.52	91.13	68.57
	Zeta (mV)			2.91	5.65	-2.50	4.20	-24.17	-45.83	-29.17	-46.67	-44.23		-11.77	-0.18	-32.60	-41.03	-21.47	-14.73
1 mM	Size (nm)	-	-	-	-	-	-	-	-	-	-	89.03	47.42	-	-	-	-	-	-
	Zeta (mV)											-43.53	-44.40						
10 mM	Size (nm)	-	-	-	-	-	314.93	-	-	-	47.99	133.83	46.64	-	296.87	-	47.13	-	-
	Zeta (mV)						5.87				-40.83	-39.83	-44.30		8.03		-27.80		

Figure 1: *Time dependent aggregation of AuNPs functionalised with TPh 1 µM (a) and of AgNPs grafted with TPh 50 µM (b). The insert in a) presents an enlargement of the spectra. The spectral region surrounded by the dotted rectangle in a) is enlarged to highlight the low spectral intensity obtained until 30 min.*

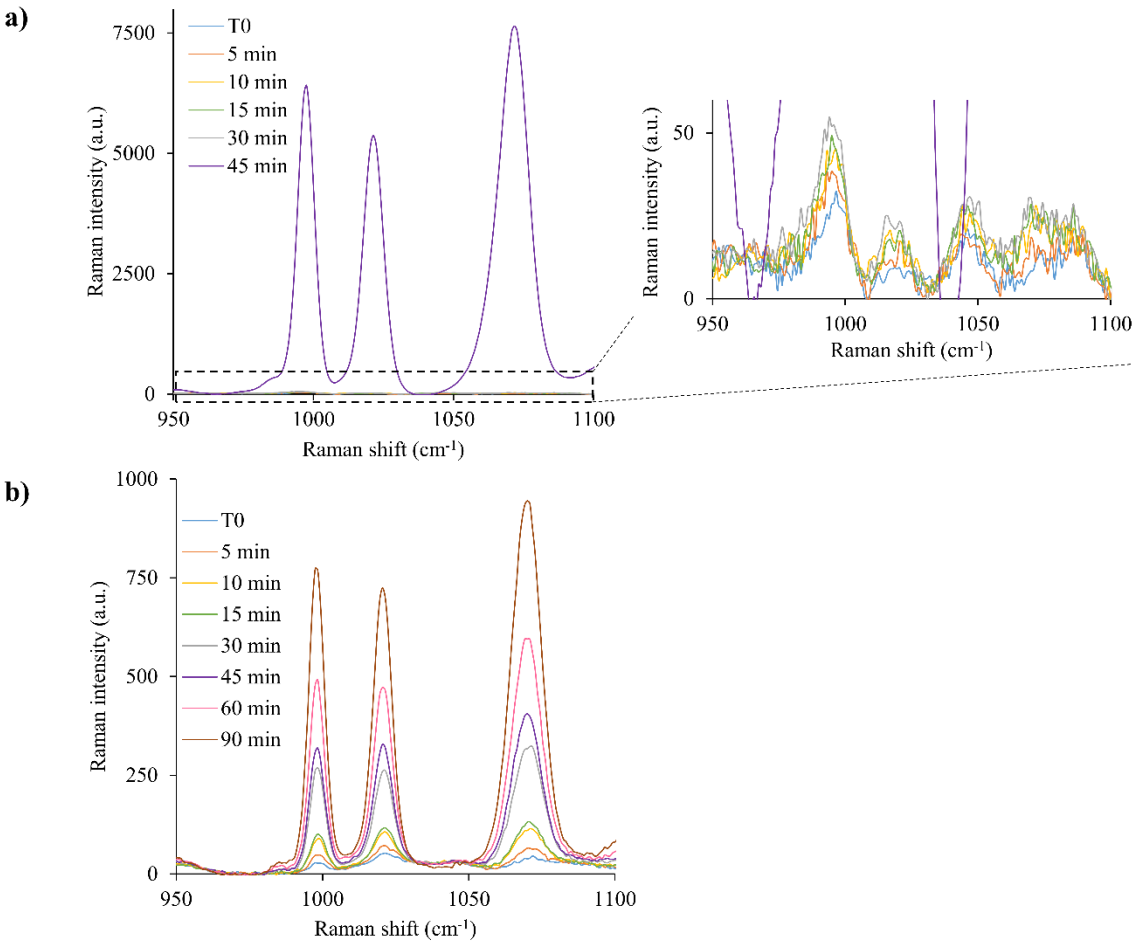

Figure 2: *Comparison of the SERS spectra of 100 µM aqueous 2-MP adsorbed onto AgNPs (pH 8) and onto AuNPs (pH 5.5). The asterisks evidence bands affected by the pH.*

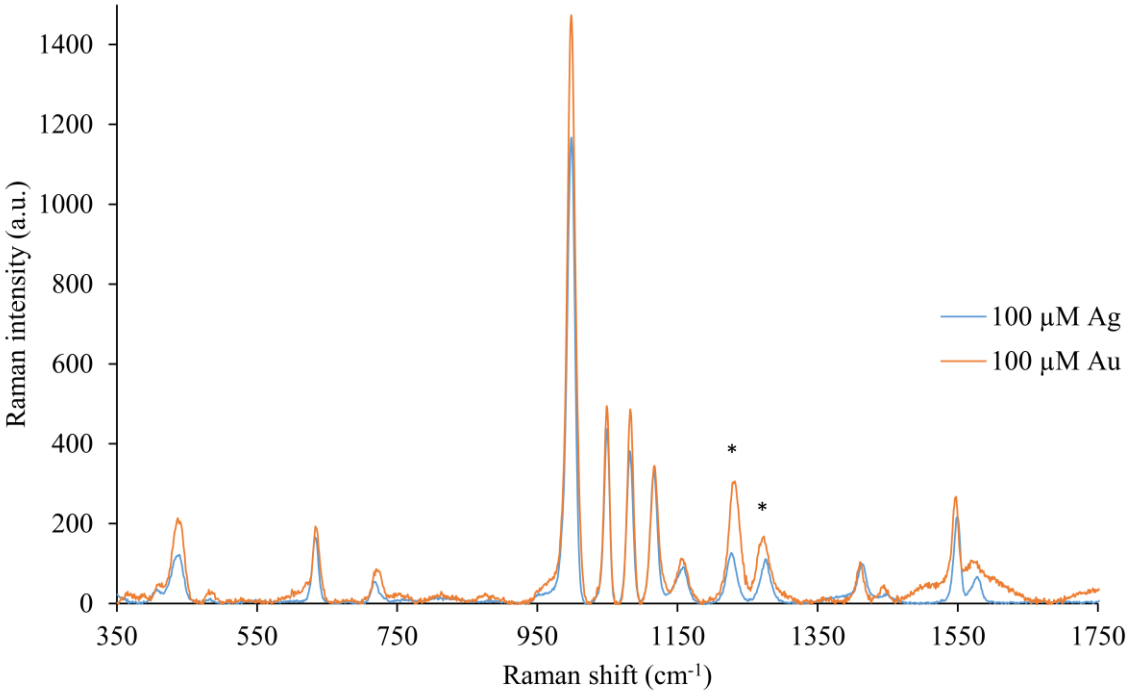

Figure 3: *Comparison of the SERS spectra of 100 µM aqueous 4-MP adsorbed onto AgNPs (pH 8) and onto AuNPs (pH 5.5). Due to the lower intensity of the spectrum of 4-MP adsorbed onto AgNPs, a normalisation of the spectrum area to the unit has been performed to compare AgNPs and AuNPs. This normalisation explains why the spectrum of 4-MP on AgNPs is noisier than that of 4-MP on AuNPs. The asterisks evidence bands affected by the pH.*

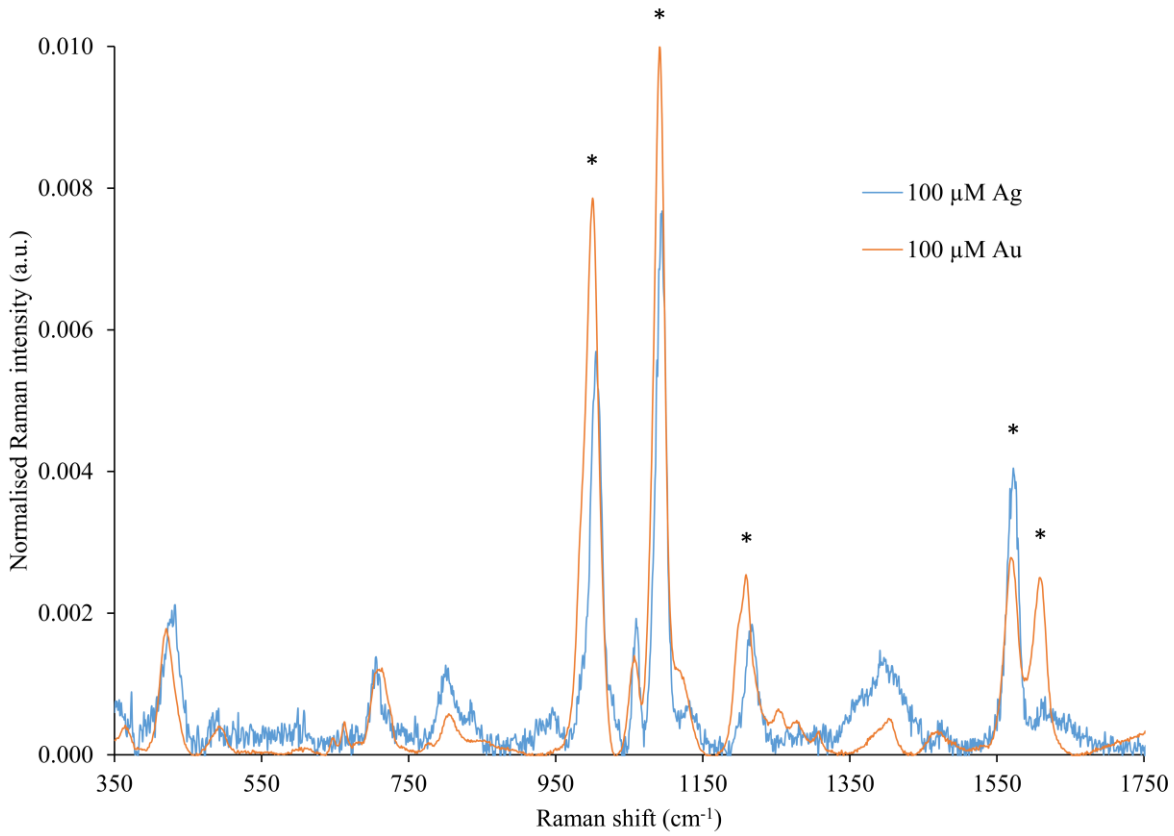

Figure 4: *Evolution over time of the UV-Visible spectra of 2-MP (a) and 4-MP (b) stored at room temperature and in the sunlight. The plain and dashed lines represent the samples prepared in water and in methanol respectively.*

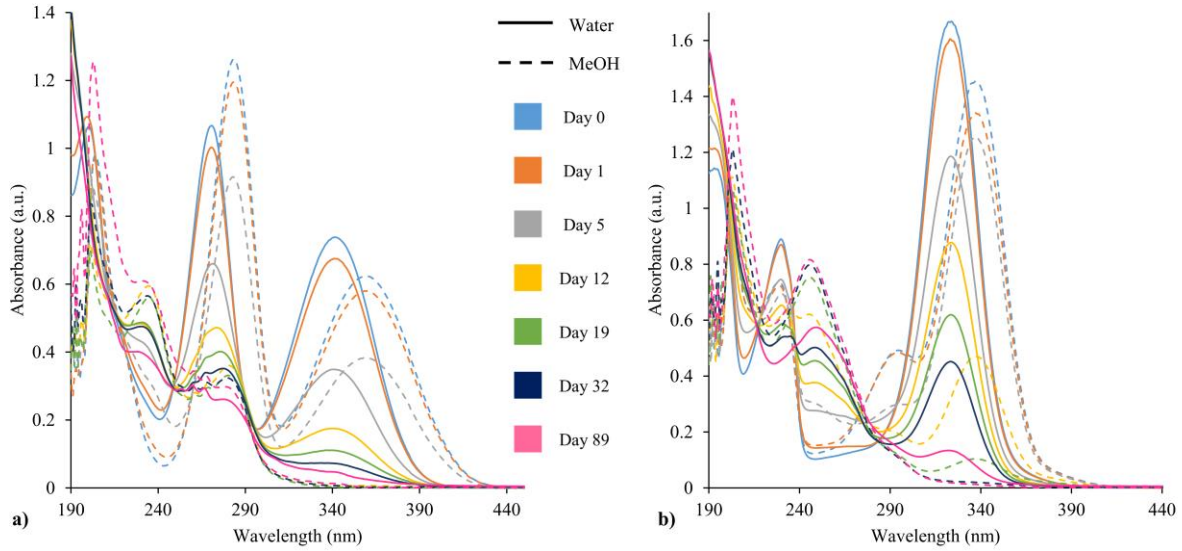

Figure 5: *SERS spectra of 100 µM methanolic 4-MP, stored during 1 month in the fridge or at room temperature, obtained with AuNPs.*

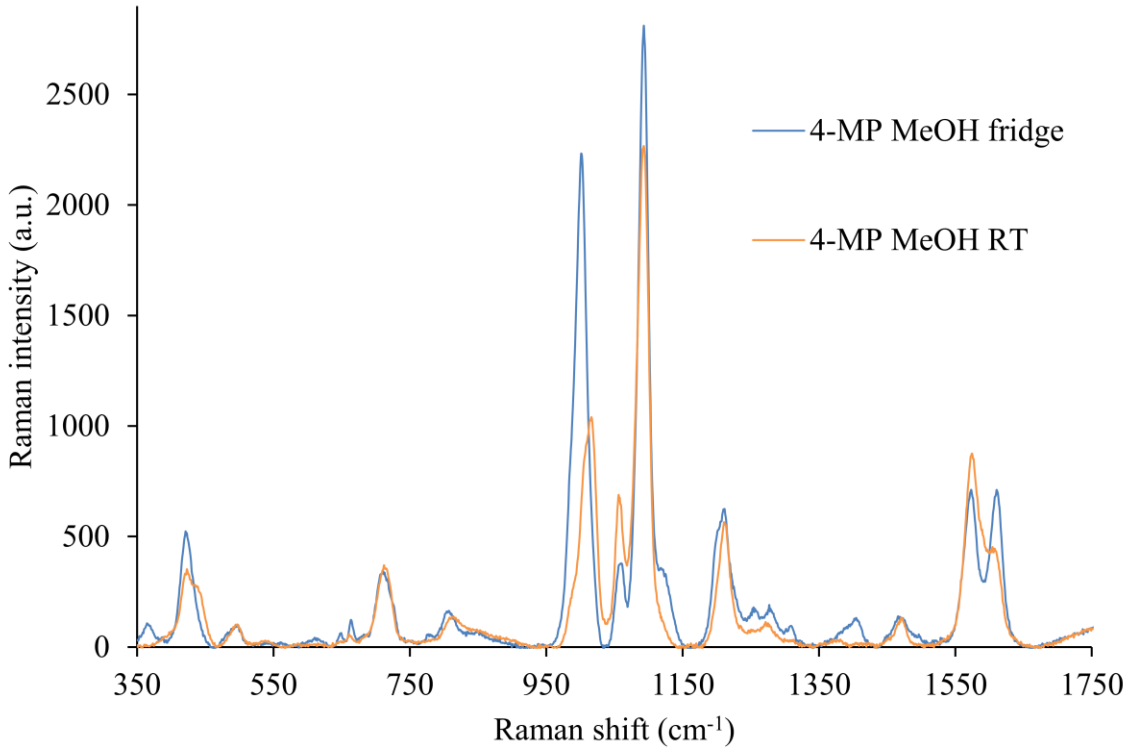

Graphical abstract:

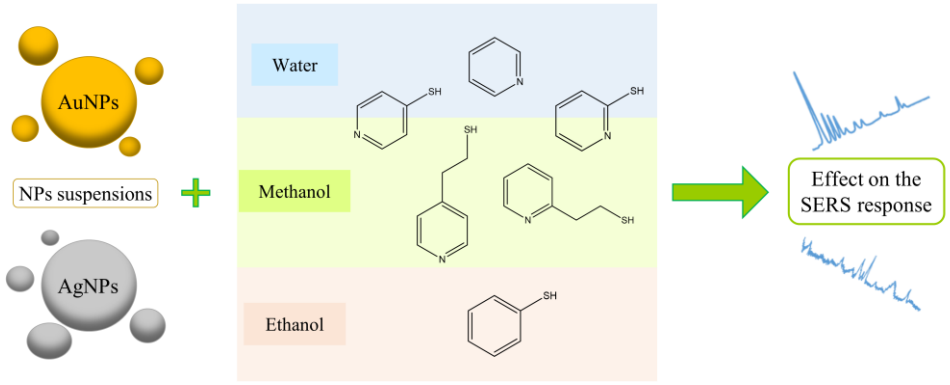

Highlights:

- The modifying agent impacts the SERS signal and the colloid aggregation state.
- pH and solvent can affect the response of SERS labels.
- The link between aggregation and SERS signal intensity was examined.
- Stability of the label must be taken into account for SERS analyses.
- DoE are beneficial for optimisation of the functionalisation agent parameters.